Rotation-induced superstructure in slow-light waveguides with mode-degeneracy: optical gyroscopes with exponential sensitivity

Ben Z. Steinberg, Jacob Scheuer,* and Amir Boag

School of Electrical Engineering, Tel Aviv University, Ramat-Aviv, Tel-Aviv 69978, Israel

Received September 5, 2006; accepted December 11, 2006;
posted January 9, 2007 (Doc. ID 74735); published April 17, 2007

We study wave propagation in a rotating slow-light structure with mode degeneracy. The rotation, in conjunction with the mode degeneracy, effectively induces superstructure that significantly modifies the structure's dispersion relation. It is shown that a rotation-dependent stop band is formed in the center of the slow-light waveguide transmission curve. A light signal of frequency within this stop band that is excited in a finite-length section of such a waveguide decays exponentially with the rotation speed and with the coupled resonator optical waveguide's total length or total number of degenerate microcavities. This effect can be used for optical gyroscopes with exponential-type sensitivity to rotation.

OCIS codes: 120.5790, 230.5750.

1. INTRODUCTION

An electromagnetic wave propagating along a circular path in a rotating medium accumulates additional phase shift that depends on the relation between the directions of the wave propagation and the medium rotation. This phase shift, known as the Sagnac effect, was recently studied in slow-wave structures consisting of a set of coupled nondegenerate microcavities.[1] This study reveals a novel manifestation of the Sagnac effect, expressed via a new (to the best of our knowledge), rotation-dependent dispersion relation. In another work,[2] the application of a microring based coupled resonator optical waveguide (CROW) for rotation sensing was studied, demonstrating a potential for significant sensitivity enhancement compared to the conventional Sagnac loops. Unlike the photonic crystal (PhC) cavities employed in Ref. 1, microrings possess mode degeneracy [clockwise (CW) and counter clockwise (CCW) propagating modes with the same resonant frequency]. Under rotation, this difference has far-reaching ramifications on the underlying physics governing the entire CROW structure, a phenomenon that was left unexplored in Ref. 2. Here we study the impact of mode degeneracy on the characteristics of rotating CROW structures. We reveal a novel effect: due to mode degeneracy, a rotation-induced superstructure emerges in the CROW, resulting in the appearance of an additional forbidden gap in the center of the dispersion curve. In addition, our analysis is general and applies also to less transparent cases of mode degeneracy such as those encountered in the PhC under rotation.[3,4]

A simple example of a resonator having degenerate modes is the microring: two modes $\mathbf{H}_0^{\pm}$ propagating in opposite directions possess the same resonance frequency ω_0. If a ring of radius R rotates at an angular velocity Ω around an arbitrary axis normal to the ring plane, ω_0 splits into two frequencies $\omega_{\pm}=\omega_0\pm\Omega\omega_0 R/nc$ due to the classical Sagnac effect[5] (see Fig. 1). Although it seems to be less transparent and intuitive, exactly the same phenomenon exists in any microcavity that supports mode degeneracy, including Phc microcavities such as those reported lately[3,4] (but with more elaborate mathematics that provide the exact splitting formula). Next, consider a CROW consisting of resonators with mode degeneracy, as in Fig. 2. When stationary, the CCW mode $\mathbf{H}_0^{+}$ in even-numbered resonators essentially couples to the CW mode $\mathbf{H}_0^{-}$ in odd-numbered resonators (due to phase-matching requirement in the area between the resonators), all having the same resonance ω_0. However, when the entire structure is rotating, each microring undergoes a split of its resonant frequencies as shown in Fig. 1. Thus, the relevant resonant frequency of the nth resonator shifts to $\omega_0+(-1)^n\delta\omega(\Omega)$, so the rotation induces a periodic modulation of the CROW properties. This rotation-dependent effective periodic modulation results in the emergence of forbidden frequencies gap within the CROW's transmission curve, as with any other wave phenomenon governed by an equation with periodic coefficients. A similar superstructure may emerge in every CROW comprising resonators with mode degeneracy.[2–4]

The purpose of the present work is to study this effect analytically and to demonstrate it numerically. Furthermore, as shown in Section 3, the rotation induces a forbidden frequencies gap within the CROWs transmission curve—a regime in which propagation possesses exponential decay behavior. Thus, we show that the novel effect reported here can be used to design new devices with exponential-type sensitivity to rotation and to the CROW length. This may have important practical implications. The study is carried out in the rotating CROW rest frame, and our starting point is the set of Maxwell's equation in noninertial rotating media. After deriving the appropriate wave equations, a mathematical solution procedure based on a tight-binding approach is invoked. This approach is chosen for several reasons. It is well suited for CROW

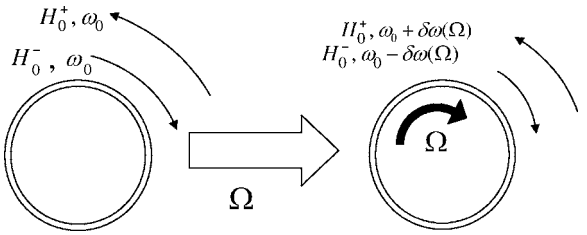

Fig. 1. Splitting of the ring degenerate modes due to rotation.

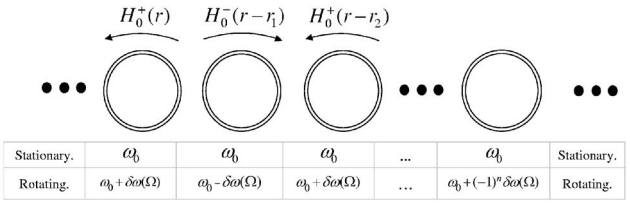

Stationary.	ω_0	ω_0	ω_0	...	ω_0	Stationary.
Rotating.	$\omega_0+\delta\omega(\Omega)$	$\omega_0-\delta\omega(\Omega)$	$\omega_0+\delta\omega(\Omega)$	...	$\omega_0+(-1)^n\delta\omega(\Omega)$	Rotating.

Fig. 2. Stationary and rotating CROW consisting of ring resonators.

structures consisting of weakly coupled resonators, which is the case of interest here. It simplifies the analysis by expressing many of the important quantities involved in terms of the system's basic building block: the single isolated and stationary microcavity. This simplification is also helpful in conveying clear physical interpretations. As the tight binding is based on the properties of the single microcavity, and since in our case this microcavity possesses mode degeneracy and is rotating, our analysis here uses extensively some previously developed results on the subject.[3,4] A short summary of the important points is provided here where needed, and the reader is referred to our previous works[3,4] for their derivations. It is recognized that other mathematical approaches, such as the transfer matrix method,[2] may provide solutions that are valid beyond the tight-binding regime. However, we believe that the basic properties of the novel effect reported here, as well as many of the computational results pertaining to the new dispersion relations, are, in principle, valid beyond the tight-binding approximation. Furthermore, the tight-binding approach can be used in a more general context where the microcavities modes cannot be described by a simple local plane wave, as done in the transfer matrix approach.

Finally, a short comment regarding terminology is in order. In previous publications pertaining to propagation in stationary or rotating sets of microcavities, and especially in a previous work related to rotating PhCs,[1] the authors used the term "coupled cavity waveguide"—CCW. This is quite unfortunate due to the ambiguity with the term "counterclockwise" (CCW) used to define a direction of rotation. Thus, in this work we use the term CROW to designate the system consisting of a set of microcavities, and we use the terms CW and CCW to designate rotation directions.

The structure of the paper is as follows. In Section 2, we provide a brief overview of the mathematical and physical properties of a single rotating microcavity. This overview summarizes the results of a previous study by the authors[3,4] that are needed here in order to construct the appropriate tight-binding solution procedure. In Section 3, we derive the basic wave equations governing the rotating CROW, as seen in the CROW rest frame, and solve the equations using an appropriate extension of tight-binding theory. The general form of the dispersion relation is exposed and discussed. In Section 4, we provide numerical examples that demonstrate the properties developed analytically. Concluding remarks are provided in Section 5.

2. DEGENERATE MODES IN A SINGLE STATIONARY OR ROTATING MICROCAVITY: AN OVERVIEW

Before analyzing the effect of rotation on the entire structure of a CROW made of degenerate modes microcavities, it is instructive to discuss in more detail the effect of rotation on a single microcavity that supports degenerate modes. We summarize here the main results of one of our previous studies,[3,4] with emphasis on the points that are of most relevance to the present study. We consider first the stationary case, and start with the wave equation for the magnetic field modes of a general resonator supporting M degenerate modes that resonate at frequency ω_0. Denote the degenerate modes by $\mathbf{H}_0^{(m)}(\mathbf{r})$, $m=1,2,\ldots,M$. When the system is at rest, these modes satisfy

$$\mathbf{\Theta}_d \mathbf{H}_0^{(m)}(\mathbf{r}) = k_0^2 \mathbf{H}_0^{(m)}(\mathbf{r}), \quad k_0 = \omega_0/c, \quad m = 1,2,\ldots,M, \tag{2.1}$$

where $\mathbf{\Theta}_d$ is the wave operator:

$$\mathbf{\Theta}_d \equiv \nabla \times \frac{1}{\epsilon_d(\mathbf{r})} \nabla \times . \tag{2.2}$$

Here $k_0=\omega_0/c$ where c is the vacuum speed of light, and $\epsilon_d(\mathbf{r})$ is the relative dielectric structure of the single resonator. As pointed out in Section 1, for the specific case of a ring resonator we have only two degenerate modes, so $M=2$. These two degenerate modes can be cast in many different ways. Denoting the arc length along the ring periphery and the corresponding propagation constant (wavenumber) by s and β, respectively, the modes can be defined as the two standing waves $\cos(\beta s)$ and $\sin(\beta s)$. Alternatively they can be rewritten as the two propagating waves $e^{i\beta s}$ and $e^{-i\beta s}$. Since any linear combination of degenerate modes is by itself a degenerate mode, these two representations are formally equally legitimate, as well as infinitely many other linear combinations. However, with respect to rotation problems, what signifies the propagating waves representation ($e^{\pm i\beta s}$) is the fact that their spatial form is unchanged under rotation. Only their resonances are changed (to $\omega_\pm=\omega_0\pm\Omega\omega_0 R/nc$, the Sagnac effect). Thus, for the ring structure, the specific form $e^{\pm i\beta s}$constitutes the rotation eigenmodes. We denote them here by $\mathbf{H}_\Omega^\pm$. Note that these modes are orthogonal.

It turns out that a similar situation exists in *any* rotating cavities that support mode degeneracy, even if the corresponding modal shapes are not as transparent and obvious as those of the ring.[3,4] This includes, as a special case, degenerate modes microcavities formed by local defects in PhCs.[6,7] Suppose the stationary cavity possesses two degenerate modes $\mathbf{H}_0^{(1,2)}$. Without loss of generality,

they can be assumed mutually orthonormal (every linear combination of degenerate modes is a degenerate mode; thus, if one starts with fields that are not orthonormal, Gram–Schmidt orthogonalization can be applied, and the end result would be an orthonormal pair of degenerate modes). Then the two unique linear combinations,

$$\mathbf{H}_{\Omega}^{\pm} = \sum_{m=1}^{2} a_m^{\pm} \mathbf{H}_0^{(m)}, \quad a_2^{\pm} = \pm i a_1^{\pm}, \tag{2.3}$$

result in fields $\mathbf{H}_{\Omega}^{\pm}$ that constitute the rotation eigenmodes. These modes possess the following important properties pertaining to both the stationary and the rotating cavity[3,4]:

(i) They are orthonormal $\langle \mathbf{H}_{\Omega}^{+}, \mathbf{H}_{\Omega}^{-} \rangle = 0$ [see Eq. (3.12) for the definition of the inner product].

(ii) Since they are given by linear combinations of degenerate modes of the stationary system Eq. (2.1), they as well constitute degenerate modes of the stationary system, satisfying

$$\mathbf{\Theta}_d \mathbf{H}_{\Omega}^{\pm}(\mathbf{r}) = k_0^2 \mathbf{H}_{\Omega}^{\pm}(\mathbf{r}), \tag{2.4}$$

(iii) These rotation eigenmodes $\mathbf{H}_{\Omega}^{\pm}$ are themselves rotating fields, just like their celebrated cousins $e^{\pm i\beta s}$ [note the $\pi/2$ phase difference between the summation amplitudes in Eq. (2.3), and the fact that the summed fields $\mathbf{H}_0^{(1,2)}$ are orthonormal].

(iv) Their spatial form stays unchanged under physical rotation of the system (as seen in the rotating system rest frame).

(v) Under rotation, their corresponding resonance frequencies as measured in the rotating system rest frame are obtained by the splitting formula

$$\omega_{\pm} = \omega_0 \pm \delta\omega(\Omega), \quad \delta\omega(\Omega) = \omega_0 \Omega \Lambda. \tag{2.5}$$

Here Ω is the rotation angular velocity, and Λ is the eigenvalue of an appropriately defined rotation operator.

(vi) $\mathbf{H}_{\Omega}^{\pm}$ constitute the eigenmodes of the wave equation governing the fields in the rotating system rest frame, with eigenvalues given by the splitting formula above. In fact, properties (iv) and (v) are nothing but a manifestation of this general fact.[3,4] Furthermore, for slow rotations these results are independent of the location of the rotation axis.

It has been shown[4] that the above properties are general and hold for any microcavity with mode degeneracy. For the case of a simple closed-loop resonator, they boil down to the classical Sagnac effect.

Before concluding this section, it is instructive to show a specific example. Consider a two-dimensional PhC that consists of dielectric cylinders of radius 0.6 μm and $\epsilon_r = 8.41$, situated on a hexagonal lattice with lattice constant of $a = 4$ μm. For TM polarization, a microcavity with two degenerate modes at a resonant wavelength of $\lambda_0 = 2\pi c/\omega_0 = 8.79941$ μm is created by increasing the radius of a cylinder to 1.1 μm. Two possible sets of the degenerate modes electric field magnitude is shown in a logarithmic scale in Fig. 3. The rotation eigenmodes for this system are obtained by substituting the orthogonal version of the set [shown in Figs. 3(c) and 3(d)] into the summation in Eq. (2.3). The resulting eigenmodes shapes evolve gradually from the shape shown in Fig. 3(c) at, say, $t = 0$ to the shape shown in Fig. 3(d) at $\omega t = \pi/2$ and back, perpetually. The results are two modes of identical spatial forms shown in Fig. 4, rotating around the cavity center in mutually opposite directions. Clearly, if two neighboring microcavities of this type (i.e., each of them supports

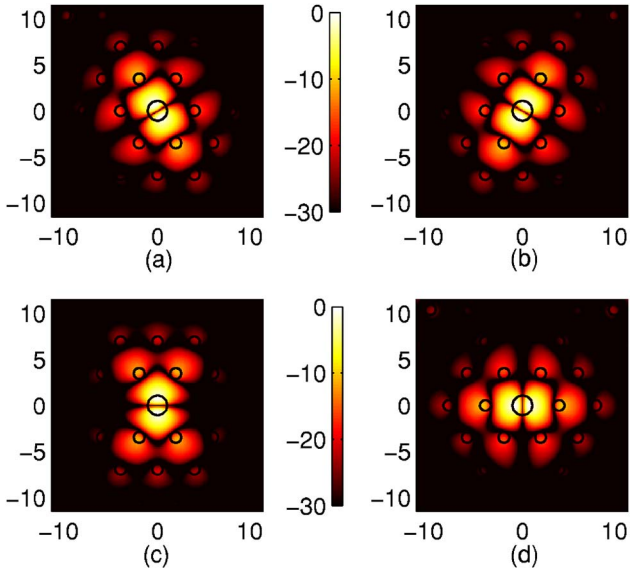

Fig. 3. (Color online) Electric field magnitudes in decibel scale of a doubly degenerate TM microcavity ($M = 2$), in a 2D hexagonal PhC. The crystal is made of dielectric cylinders, outlined by the black circles. (a) $\mathbf{E}_0^{(1)}$. (b) $\mathbf{E}_0^{(2)}$. These modes are nonorthogonal, and $\mathbf{E}_0^{(2)}$ is a $\pi/3$-rotated replica of $\mathbf{E}_0^{(1)}$. (c) The linear combination $\mathbf{E}_0^{(1)} \mapsto \mathbf{E}_0^{(1)} + \mathbf{E}_0^{(2)}$. (d) The linear combination $\mathbf{E}_0^{(2)} \mapsto \mathbf{E}_0^{(1)} - \mathbf{E}_0^{(2)}$. These modes are orthogonal.

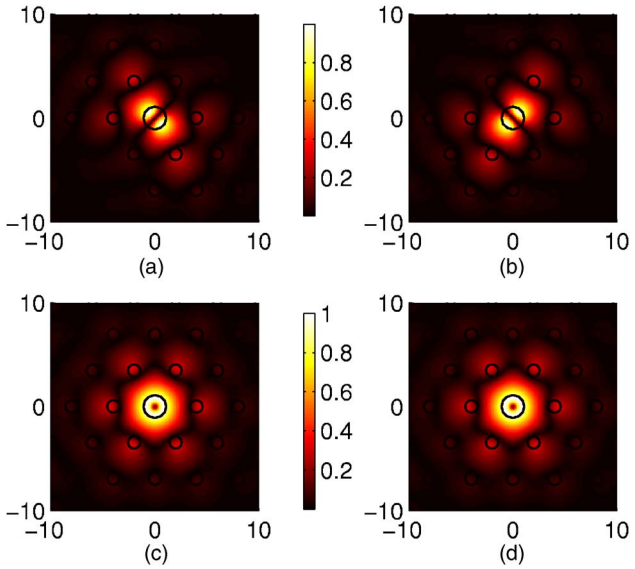

Fig. 4. (Color online) Electric field of the rotation eigenmodes associated with the PhC microcavity of Fig. 3. The two modes have exactly the same spatial form shown here. $\mathbf{E}_{\Omega}^{+}$, $\mathbf{H}_{\Omega}^{+}$ rotate CW and $\mathbf{E}_{\Omega}^{-}$, $\mathbf{H}_{\Omega}^{-}$ rotate CCW. They are obtained by the linear combination in Eq. (2.3), using the orthogonal pair shown in Figs. 3(c) and 3(d). All quantities are shown on linear scale. (a) The instantaneous field $|\Re\epsilon(\mathbf{E}_{\Omega}^{-} e^{i\omega t})|$ for $\omega t = \pi/4$. (b) The same as (a), but for $\mathbf{E}_{\Omega}^{+}$. (c) $|\mathbf{E}_{\Omega}^{-}|$. The rotating field forms a ring along which the field power propagates. (d) $|\mathbf{E}_{\Omega}^{+}|$.

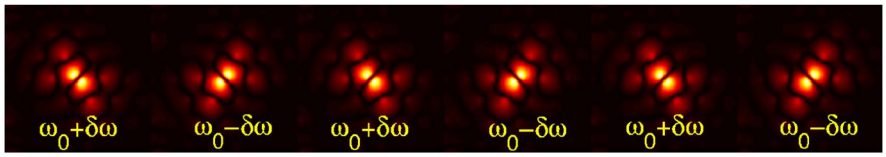

Fig. 5. (Color online) Instantaneous field of a degenerate modes CROW, made of a set of equally spaced PhC microcavities such as the one discussed in Figs. 3 and 4. Counting from left, the modes in the odd- (even-) numbered cavities are rotating in a CCW (CW) direction. A rigid mechanical rotation of the entire structure in the CW direction causes the alternating of the resonance shift $\delta\omega$ that depends linearly on the rotation rate as shown in Eq. (2.5). Thus, rotation induces a modulation of the local resonance frequency, similar to the phenomenon described in Fig. 2.

two degenerate modes) are created in a PhC, the CW rotating mode in one cavity couples best to the CCW rotating mode of its neighbor. Hence, a PhC based analogy of the ring-CROW structure shown in Fig. 2, can be constructed by a set of equally spaced microcavities, each supporting two degenerate modes as discussed above. This system is shown in Fig. 5.

3. STUDY OF THE ROTATING CROW IN ITS REST FRAME OF REFERENCE

In this section, we develop the general wave equations governing the fields of rotating system (i.e., the entire CROW, made of ring resonators or PhC microcavities), as seen in the rotating medium *rest frame*, which is noninertial. Then, the tight-binding approach is employed to solve the equation and study the propagation in the rotating CROW. Let $\epsilon_r(\mathbf{r})$ be the (time-invariant) relative dielectric property of a stationary medium, as measured in its (inertial) rest frame. We assume now that the medium rotates slowly around the z axis at an angular radian velocity Ω:

$$\mathbf{\Omega} = \hat{z}\Omega. \tag{3.1}$$

The assumption of slow rotation implies that

(i) The angular velocity Ω and the PhC maximal dimension L satisfy $|\Omega L| \ll c$. Therefore no relativistic effects take place.

(ii) Consistent with the slow velocity assumption, no geometrical transformations or deformations take place. Thus, for example, the ∇ operator is conserved: $\nabla = \nabla'$. For the very same reason, time is invariant in both systems: $t = t'$.

According to a formal structure of electrodynamics, postulated in fundamental studies,[8,9] the basic physical laws governing the electromagnetic fields are invariant under *any* coordinate transformation, including a noninertial one. The transformation to a rotating system is manifested only by an appropriate change of the constitutive relations. Therefore under the slow rotation assumption discussed above, the source-free Maxwell's equations in the rotating frame $\mathcal{R}$ are given by[8,9]

$$\nabla \times \mathbf{E} = i\omega\mathbf{B}, \quad \nabla \cdot \mathbf{B} = 0, \tag{3.2a}$$

$$\nabla \times \mathbf{H} = -i\omega\mathbf{D}, \quad \nabla \cdot \mathbf{D} = 0. \tag{3.2b}$$

Let the material properties at rest be given by $\epsilon(\mathbf{r}) = \epsilon_0\epsilon_r(\mathbf{r})$, $\mu = \mu_0$. Then up to the first order in velocity the constitutive relations in $\mathcal{R}$ take on the form[8]

$$\mathbf{D} = \epsilon\mathbf{E} - c^{-2}\mathbf{\Omega} \times \mathbf{r} \times \mathbf{H}, \tag{3.3a}$$

$$\mathbf{B} = \mu\mathbf{H} + c^{-2}\mathbf{\Omega} \times \mathbf{r} \times \mathbf{E}. \tag{3.3b}$$

In the above, c is the speed of light in vacuum, ω is the frequency, and a time-dependence $e^{-i\omega t}$ is assumed and suppressed. This set of Maxwell's equations has been used in the past as the starting point for studies of the Sagnac effect in classic works on optical gyroscopes by numerous authors.[10] We now follow the procedure outlined in a previous work by one of the authors[1] to derive a wave equation governing the magnetic field. Substitute the above constitutive relations into Maxwell's equations (3.2a) and (3.2b). The result is

$$\mathcal{D} \times \mathbf{E} = i\omega\mu\mathbf{H}, \tag{3.4a}$$

$$\mathcal{D} \times \mathbf{H} = -i\omega\epsilon\mathbf{E}, \tag{3.4b}$$

where $\mathcal{D}$ is the operator:

$$\mathcal{D} \equiv \nabla - ik\boldsymbol{\beta}(\mathbf{r}), \quad k = \omega/c, \quad \boldsymbol{\beta}(\mathbf{r}) = c^{-1}\mathbf{\Omega} \times \mathbf{r}. \tag{3.5}$$

Now follow the standard procedure of deriving the wave equation for $\mathbf{H}$, with $\mathcal{D}$ replacing ∇. The resulting equation is $\mathcal{D} \times (1/\epsilon_r)\mathcal{D} \times \mathbf{H} = k^2\mathbf{H}$. Collecting terms that are first order only (with respect to velocity,) and rearranging, we end up with the new wave equation in the rotating medium rest frame, governing the magnetic field $\mathbf{H}_\Omega(\mathbf{r})$[1]:

$$\Theta\mathbf{H}_\Omega(\mathbf{r}) = k^2\mathbf{H}_\Omega(\mathbf{r}) + ik\mathbf{L}_\Omega\mathbf{H}_\Omega(\mathbf{r}). \tag{3.6a}$$

Here, Θ is the wave operator associated with the entire structure,

$$\Theta \equiv \nabla \times \frac{1}{\epsilon_r(\mathbf{r})}\nabla \times, \tag{3.6b}$$

and $\mathbf{L}_\Omega$ is the rotation-induced operator,

$$\mathbf{L}_\Omega\mathbf{H} = \nabla \times \frac{\boldsymbol{\beta}(\mathbf{r})}{\epsilon_r(\mathbf{r})} \times \mathbf{H} + \frac{\boldsymbol{\beta}(\mathbf{r})}{\epsilon_r(\mathbf{r})} \times \nabla \times \mathbf{H}, \quad \boldsymbol{\beta}(\mathbf{r}) = \mathbf{\Omega} \times \mathbf{r}/c. \tag{3.6c}$$

In developing Eqs. (3.6a), (3.6b), and (3.6c), only terms up to first order in $\boldsymbol{\beta}$ were kept.[1,8] Note that when no rotation takes place, $\mathbf{L}_\Omega$ vanishes and Eq. (3.6a) reduces to the well-known stationary medium wave equation.

We now wish to solve Eq. (3.6a) for the entire CROW under slow rotation rates (say, typical to those relevant

for optical gyroscopes; $\Omega \leq 1$ rad/s). Since the CROW consists of weakly coupled resonators, the tight-binding approach can provide a convenient solution technique. Thus, we follow the rotating-CROW solution technique developed previously[1] with the modifications needed to handle properly the microcavities mode degeneracy. Considering the general observations made in properties (iii) and (iv) in Section 2, and the fact that a CW rotating mode in a given resonator couples only to the CCW rotating mode of its neighbor, we expand the total field of the rotating system with the modes $\mathbf{H}_\Omega^\pm$,

$$\mathbf{H}_\Omega = \sum_m A_m \mathbf{H}_m(\mathbf{r}), \quad \mathbf{H}_m(\mathbf{r}) = \begin{cases} \mathbf{H}_\Omega^+(\mathbf{r}-\mathbf{r}_m) & m \text{ even} \\ \mathbf{H}_\Omega^-(\mathbf{r}-\mathbf{r}_m) & m \text{ odd} \end{cases}, \tag{3.7}$$

where $\mathbf{r}_m$ is the location of the mth resonator center. In this representation of the solution, the modal fields $\mathbf{H}_\Omega^\pm$ are used as mere building blocks, and the fact that they satisfy Eq. (2.4) will be exploited. The intercavity (weak) coupling, as well as the effect of rotation, will be manifested via the (yet unknown) expansion coefficients A_m.

We decompose now the relative dielectric property of the entire structure $\epsilon_r(\mathbf{r})$ to that of the background structure $\epsilon_b(\mathbf{r})$ (without the resonators or local defects, but *with* the perfect PhC, if the CROW is realized by array of local defects in a photonic crystal), and a series of defect contributions. Thus, $1/\epsilon_r(\mathbf{r})$ in Eq. (3.6b) can be expressed as

$$\frac{1}{\epsilon_r(\mathbf{r})} = \frac{1}{\epsilon_b(\mathbf{r})} + \sum_k d(\mathbf{r},\mathbf{r}_k), \tag{3.8a}$$

where $d(\mathbf{r},\mathbf{r}_k)$ is the variation in $1/\epsilon_r$ introduced by the kth resonator or local defect:

$$d(\mathbf{r},\mathbf{r}_k) = \frac{1}{\epsilon_d(\mathbf{r}-\mathbf{r}_k)} - \frac{1}{\epsilon_b(\mathbf{r})}. \tag{3.8b}$$

Here $\epsilon_d(\mathbf{r})$ represents the perfect background with a single resonator or a local defect, located at the origin. With this decomposition the operator $\boldsymbol{\Theta}$ is decomposed into a series of operators representing the contribution of the background structure and of each of the resonators (or local defects) separately,

$$\boldsymbol{\Theta} = \boldsymbol{\Theta}^b + \sum_k \boldsymbol{\Theta}_k, \tag{3.9a}$$

where

$$\boldsymbol{\Theta}^b = \boldsymbol{\nabla} \times \frac{1}{\epsilon_b(\mathbf{r})} \boldsymbol{\nabla} \times, \quad \boldsymbol{\Theta}_k = \boldsymbol{\nabla} \times d(\mathbf{r},\mathbf{r}_k) \boldsymbol{\nabla} \times. \tag{3.9b}$$

Due to the property (ii) in Section 2, and Eq. (2.4), each of the summed modes $\mathbf{H}_m$ in Eq. (3.7) satisfies

$$(\boldsymbol{\Theta}^b + \boldsymbol{\Theta}_m)\mathbf{H}_m = \left(\frac{\omega_0}{c}\right)^2 \mathbf{H}_m. \tag{3.10}$$

This decomposition will be used in subsequent derivations.

We now wish to obtain the rotating CROW solution by solving for the expansion coefficients A_m in Eq. (3.7). Note that Eq. (3.6a) is not self-adjoint, thus the standard variational procedure for determining the set of A_m does not hold here. Instead, we adopt the projection approach.[1] We first substitute the expansion in Eq. (3.7) into the wave equation (3.6a) and perform an inner product of the resulting equation with $\mathbf{H}_n$, with n roaming over all the resonators involved (this amounts to the requirement that the residual error associated with the solution be orthogonal to the solution building blocks). The result is the following algebraic set of equations for the coefficients A_m:

$$\sum_m A_m \langle \boldsymbol{\Theta}\mathbf{H}_m, \mathbf{H}_n \rangle = k^2 \sum_m A_m \langle \mathbf{H}_m, \mathbf{H}_n \rangle + ik \sum_m A_m \langle \mathbf{L}_\Omega \mathbf{H}_m, \mathbf{H}_n \rangle. \tag{3.11}$$

Here $\langle \mathbf{F}, \mathbf{G} \rangle$ is the inner product

$$\langle \mathbf{F}, \mathbf{G} \rangle \equiv \int \mathbf{F} \cdot \bar{\mathbf{G}} \mathrm{d}^3\mathbf{r}, \quad \langle \mathbf{F}, \mathbf{F} \rangle = \|\mathbf{F}\|^2, \tag{3.12}$$

where the overbar denotes the complex conjugate, and $\mathbf{F} \cdot \mathbf{G}$ is the standard scalar product between the two vectors $\mathbf{F}$ and $\mathbf{G}$. Note that since the indices m, n indicate resonator locations, and since the modal fields in each resonator are tightly confined, we can approximate the first inner product in the right-hand side of Eq. (3.11) by $\delta_{mn}\|\mathbf{H}_\Omega^+\|^2$. Using this approximation, substituting the operator decomposition in Eqs. (3.9a) and (3.9b) into Eq. (3.11), and using Eq. (3.10), we obtain

$$(k_0^2 - k^2)\|\mathbf{H}_\Omega^+\|^2 A_n + \sum_m \tau_{m-n} A_m - ik \sum_m \langle \mathbf{L}_\Omega \mathbf{H}_m, \mathbf{H}_n \rangle A_m = 0. \tag{3.13}$$

Here τ_{m-n}, obtained and used in numerous other studies pertaining to tight-binding analysis of CROWs[1,11,12] is given by

$$\tau_{m-n} = \left\langle \sum_{k \neq m} \boldsymbol{\Theta}_k \mathbf{H}_m, \mathbf{H}_n \right\rangle. \tag{3.14}$$

It has been shown[11] that for $m-n \neq \pm 1$, these elements are exponentially small compared to the dominant elements $\tau_1 = \tau_{-1}$.

Finally, the inner products in the rightmost summation in Eq. (3.13) can be simplified considerably. Following the same steps used in a previous work on the subject,[1] with the slight generalization needed here (in Ref. 1 the modes are assumed to be real), we obtain (see Appendix A for derivation):

$$\langle \mathbf{L}_\Omega \mathbf{H}_m, \mathbf{H}_n \rangle = ic^{-1}\Omega\omega_0\epsilon_0 \langle \rho\hat{\phi}, \bar{\mathbf{H}}_m \times \mathbf{E}_n + \mathbf{H}_n \times \bar{\mathbf{E}}_m \rangle. \tag{3.15}$$

This quantity is independent of the origin location (and rotation axis) with respect to the cavity location. Note that the modal fields $\mathbf{E}_m$, $\mathbf{H}_m$ are tightly localized within the mth cavity, and they decay exponentially away from it. Thus, under the tight-binding approximation the last equation yields

$$\langle \mathbf{L}_\Omega \mathbf{H}_m, \mathbf{H}_n \rangle \to \begin{cases} 0 & m \neq n \\ -i2\Omega k_0 \epsilon_0 \langle \rho \hat{\phi}, \Re\mathrm{e}\mathcal{S}_m \rangle & m = n \end{cases}, \tag{3.16}$$

where $\mathcal{S}_m$ is the Poynting vector carried by the rotation eigenmode in the mth cavity,

$$\mathcal{S}_m \equiv \mathbf{E}_m \times \bar{\mathbf{H}}_m = -\mathcal{S}_{m-1} = (-1)^m \mathcal{S}_0. \tag{3.17}$$

The alternating behavior follows from the definition of $\mathbf{E}_m, \mathbf{H}_m$ in Eq. (3.7) and from the fact that the modal fields $(\mathbf{E}_\Omega^+, \mathbf{H}_\Omega^+)$ rotate in opposite direction to the modal fields $(\mathbf{E}_\Omega^-, \mathbf{H}_\Omega^-)$. The $m=n$ elements of Eq. (3.16) can now be rewritten as

$$\langle \mathbf{L}_\Omega \mathbf{H}_m, \mathbf{H}_m \rangle = 2ic^{-1} \|\mathbf{H}_\Omega^+\|^2 (-1)^m \delta\omega(\Omega),$$
$$\delta\omega(\Omega) = -\Omega\omega_0 \epsilon_0 \langle \rho\hat{\phi}, \Re\mathrm{e}\mathcal{S}_0 \rangle, \tag{3.18}$$

where, surprisingly, the quantity $\delta\omega(\Omega)$ is identical to the frequency splitting of doubly degenerate modes in a single (completely isolated) rotating microcavity[4] (and it has also been shown that this expression reduces to the classical Sagnac effect if the microcavity consists of a simple closed loop).

Collecting and substituting the last results into the matrix in Eq. (3.13) we obtain [assume that the operating frequency ω is very close to the stationary cavity resonance $\omega \approx \omega_0$, so $\omega_0^2 - \omega^2 \approx 2\omega_0(\omega_0 - \omega)$],

$$\frac{\Delta\omega}{2}(A_{n-1} + A_{n+1}) + (-1)^n \delta\omega(\Omega) A_n = (\omega - \omega_0) A_n, \tag{3.19a}$$

where $\Delta\omega$ is the stationary CROW bandwidth given by

$$\Delta\omega = \frac{c^2 \tau_1}{\omega_0 \|\mathbf{H}_\Omega{}^+\|^2}. \tag{3.19b}$$

The last result can be rewritten as a matrix equation:

$$\begin{bmatrix} \vdots & \vdots & \vdots & \vdots & \vdots & \vdots & \vdots & & \\ \cdots & 0 & 0.5 & \frac{\delta\omega(\Omega)}{\Delta\omega} & 0.5 & 0 & \cdots & & \\ & \cdots & 0 & 0.5 & -\frac{\delta\omega(\Omega)}{\Delta\omega} & 0.5 & 0 & \cdots & \\ & & \cdots & 0 & 0.5 & \frac{\delta\omega(\Omega)}{\Delta\omega} & 0.5 & 0 & \cdots \\ & & & \cdots & 0 & 0.5 & -\frac{\delta\omega(\Omega)}{\Delta\omega} & 0.5 & 0 & \cdots \\ & & & \vdots & \vdots & \vdots & \vdots & \vdots & \vdots & \vdots \end{bmatrix} \mathbf{A} = \frac{\omega - \omega_0}{\Delta\omega} \mathbf{A}. \tag{3.20}$$

This equation is nothing but an eigenvector and eigenvalue problem for the vector of coefficients A_n, and for the eigenfrequency ω of the entire CROW (more precisely, the normalized distance of ω from the stationary single-cavity resonance ω_0). For stationary CROWs ($\Omega=0$), we have from Eq. (3.18) $\delta\omega(\Omega)=0$, and the equation above reduces to the well-known eigenvalue problem treated in many other works[11] and books (Chapter 4 in Ref. 13). Expressing the eigenvector elements A_n as

$$A_n = A_0 e^{i\beta n}, \tag{3.21}$$

one obtains the celebrated stationary CROW dispersion relation:

$$\omega = \omega_0 + \Delta\omega \cos(\beta). \tag{3.22}$$

For the rotating CROW, it is seen from Eq. (3.19a) that the mode degeneracy causes a rotation-induced modulation $(-1)^n \delta\omega(\Omega)$ of the matrix coefficients. That is, one encounters now an equation with periodic coefficients, the magnitude of which is linearly dependent on the rotation angular speed Ω, with a proportionality factor that depends on the properties of the individual (doubly degenerate) microcavity. This is the mathematical manifestation of the effects discussed qualitatively in Section 1 and in Section 2 (see also Figs. 2 and 5). As we show in Section

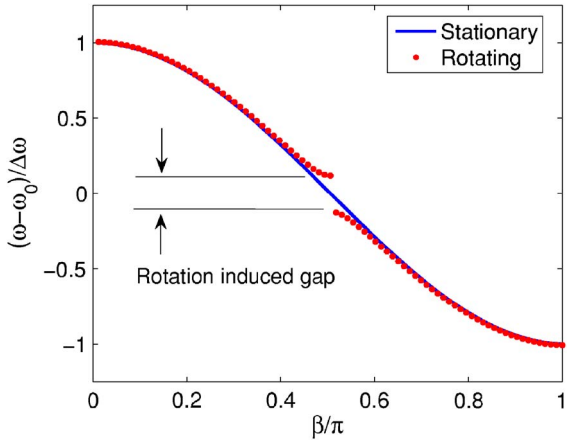

Fig. 6. (Color online) Normalized dispersion relation for stationary and rotating CROWs. For the rotating CROW we used $\delta\omega(\Omega)=0.1\Delta\omega$. This value is chosen in order to get a good graphical resolution of the effect.

4, this periodic modulation opens a rotation-dependent gap in the center of the CROW transmission curve (see Fig. 6). By solving Eq. (3.20) for the eigenvalues, it is verified that the bandwidth $\Delta\omega_r$ of the rotation-dependent gap opened in the center of the CROW transmission line is exactly the rotation-dependent splitting

$$\Delta\omega_r = \delta\omega(\Omega). \tag{3.23}$$

Furthermore, as the range above signifies the structure stop band, it is clear that an excitation of the structure by a light with frequency within this stop band, will result in an exponentially decreasing (with distance) signal. The rate of exponential decay depends on the distance of the excitation frequency from the stop-band ends, thus it increases as the rotation frequency Ω increases. This is demonstrated numerically in Section 4.

4. EXAMPLES

As pointed out before, the eigenvalues of the matrix in Eq. (3.22) can be evaluated analytically for $\delta\omega(\Omega)=0$. For the $N\times N$ matrix, the result is[13] $\lambda_k=-\cos[k\pi/(N+1)]$, $k=1,2,\ldots,N$. This is nothing but a finite-length version of the dispersion relation in Eq. (3.22) that pertains to infinitely long CROWs. Interestingly, the presence of the alternating term $(-1)^n\delta\omega(\Omega)$ on the diagonal, "clears out" the eigenvalues from the interval $[-\delta\omega(\Omega),\delta\omega(\Omega)]$, and thus it opens a gap of forbidden frequencies: $\Delta\omega_r$ in Eq. (3.23). An example is shown in Fig. 6, where the above equation has been solved for 100 resonators, and for $\delta\omega(\Omega)/\Delta\omega=0.1$. We have repeated this simulation for other values of $\delta\omega(\Omega)/\Delta\omega$, ranging from 10^{-5} to 0.5, and for N ranging from 30 to 1000, and the opening of a forbidden frequency gap with the width given by Eq. (3.23) was consistently observed.

These (normalized) results hold for *any* CROW with mode degeneracy. The parameter that characterizes a specific CROW is the sensitivity of splitting with respect to rotation, that is the function $\delta\omega(\Omega)=\Lambda\Omega$. It is important to emphasize that this function is an intrinsic property of the individual microcavity.[4] For the PhC based degenerate CROW discussed in Section 2, this function has been fully characterized previously,[4] and is given by $\delta\omega(\Omega)=0.23\,\Omega$. The stationary CROW bandwidth $\Delta\omega$ is determined solely by the intercavity spacing (under-tight-binding approximation), and in principle, it can be made arbitrarily small. Values of $\Delta\omega=10^{-5}\omega_0$ can be achieved by setting the intercavity spacing to about four crystal periods.[12]

Next we examine the transmission curve of a finite length degenerate CROW as a function of frequency, and for various values of the rotation velocity Ω. Consider a line as shown in Fig. 2, consisting of 29 ring resonators with a radius of 25 μm each, made of a dielectric material with $\epsilon=2.25$. The rings are situated along a straight path, with an intercavity coupling coefficient of $\kappa=0.01$ (power). The CROW input and output terminals consist of dielectric waveguides coupled, respectively, to the first ring on the left and to the last (rightmost) ring, both with coupling coefficient of 0.2 (power). The rings resonate at $\omega_0=12.16\times10^{14}$, which corresponds to the angular mode 152 with a vacuum wavelength of 1.55 μm. The splitting of each individual ring due to rotation is obtained here via the classical Sagnac effect, and is given by $\delta\omega(\Omega)=67.5\,\Omega$. A numerical simulation of the rotating structure using the transfer matrix approach,[2] was carried out. The CROW transmission as a function of ω is shown in Fig. 7 for various values of Ω. As predicted above, the rotation induces a stop band in the center of the transmission curve. The width of this band increases with Ω [see Eq. (3.23)] and one can readily verify that it matches the relation $\Delta\omega_r\approx\delta\omega(\Omega)=67.5\,\Omega$. It is also seen in the figure that the transmission values for frequencies within this stop band decrease rapidly as Ω is increased. In Fig. 8, we show the value of the transmission at the center of the rotating CROW stop band, as a function of Ω, for different CROW lengths. It is seen that the transmission decreases exponentially with Ω. The exponential decay rate, that is manifested by the slope of the straight line on a logarithmic scale, increases as the length of the CROW increases. Owing to the nature of the stop-band exponential decay,

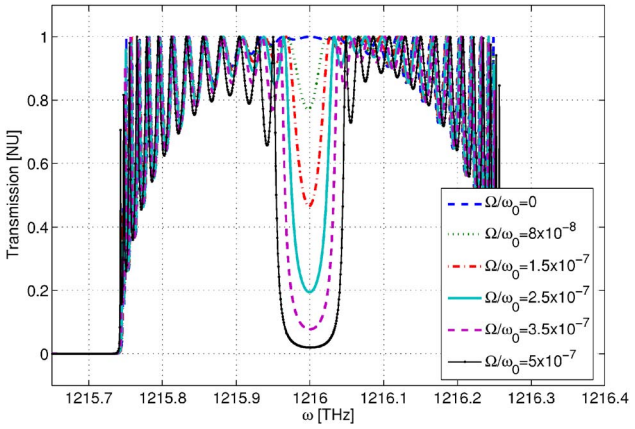

Fig. 7. (Color online) Normalized transmission for a ring resonator CROW. The rotation induces a stop band in the center of the CROW transmission curve.

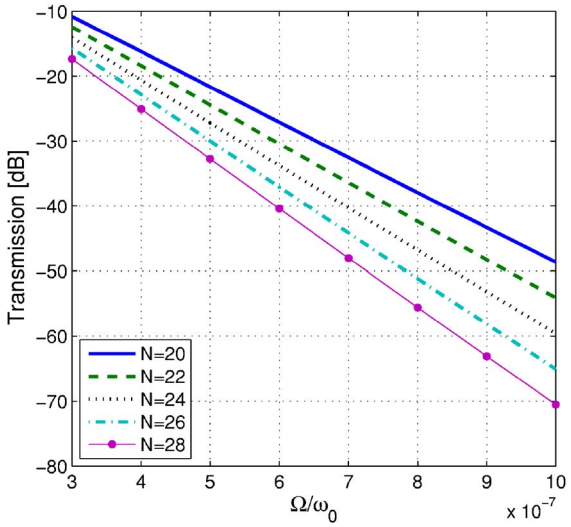

Fig. 8. (Color online) Transmission in decibels at the center of the rotating CROW stop band (i.e., at $\omega=12.16\times10^{14}$ in Fig. 7), as a function of rotation speed, and for different CROW lengths. Exponential dependence of the transmission value on Ω is evident.

the transmission of a finite-length CROW section, at the center of the stop band, can be expressed as

$$T(\omega=\omega_0,\Omega)=e^{-\alpha(\Omega/\omega_0)N}, \tag{4.1}$$

where α is a proportionality constant that depends of the CROW generic properties (microresonator properties, interresonator coupling, etc.). and N is the total number of resonators. The exponential sensitivity $dT/d(\Omega/\omega_0)/T$ is plotted in Fig. 9. As can be predicted from the exponential behavior in Eq. (4.1), the exponential sensitivity is indeed linear with the number of resonators. It should be noted that the performances predicted and verified above are independent of the general trace formed by the entire CROW; the important factors are the single microcavity properties and the total number of microcavities. This observation can be exploited for a better use of the chip area.

The results of the analysis of the rotating CROW structure sheds new light on the underlying physics of the circular gyroscope configuration studied in a previous publication.[2] Note that the number of microrings in this configuration must be odd (there is a typographical error in Fig. 3a of Ref. 2: the signal intensities for 6 and 16 microring long CROWs are actually for 5 and 15, respectively). When stationary, the index structure through which the, initially, CW mode (gray arrow in Fig. 1 of Ref. 2) propagates is identical to that encountered by the CCW mode (white arrow). However, when the CROW structure is rotating, this symmetry is broken and the two modes experience different effective structures. Assuming the CROW rotates CCW ($\Omega>0$), the CW mode experiences a sequence of microrings with alternating resonance frequencies ω_0^+, ω_0^-, ω_0^+, ω_0^-, ω_0^+,... while the CCW mode experiences the opposite sequence $-\omega_0^-$ ω_0^+, ω_0^-, ω_0^+,ω_0^-,... . As a consequence, the CW and CCW modes accumulate different phase shifts when propagating through the circular CROW, which in turn, changes the power level in the 3 dB coupler outputs. For an even number of rings, the phase responses of the effective CROW structures encountered by the CW and CCW are identical and the output signal vanishes. This argument provides an intuitive explanation to the behavior of the circular CROW gyroscope studied in Ref. 2. In particular, the phase difference between the CW and CCW propagating waves, and hence the intensity output signal, is determined directly by the number of the microrings and their radii or, equivalently, by the effective length of the CROW. This is in contrast to the conventional Sagnac effect that depends on the area circumvented by the loop.

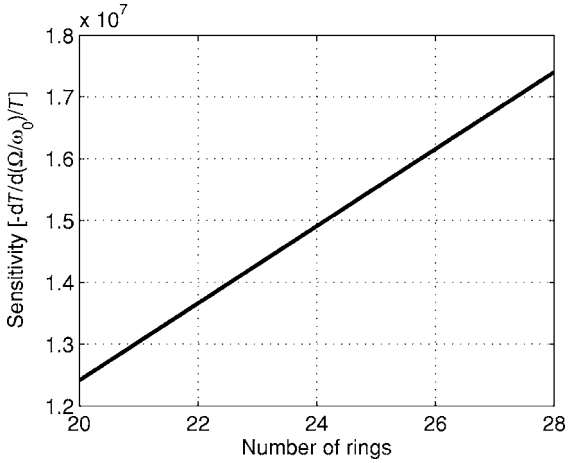

Fig. 9. Exponential sensitivity of the CROW to rotation, as a function of the CROW length (number of resonators).

5. CONCLUSIONS

Using the tight-binding approach, we have studied the effect of rotation on the CROW made of a set of microcavities with mode degeneracy. The study is carried in the rotating CROW rest frame of reference, and the results are expressed generally in terms of entities pertaining to the basic microcavity used to form the CROW, under stationary conditions. Our analysis is general and holds for any kind of microcavity with mode degeneracy: ring resonators, PhC microcavities, or disk resonators. It is shown that under rotation a superstructure emerges: rotation effectively induces a periodic modulation of the CROW properties. This fact has far reaching ramifications, as it causes the emergence of a stop band in the center of the CROW transmission band. This new effect can be used to design optical gyroscopes with exponential-type sensitivity to rotation and to the CROW's length. The sensitivity depends essentially on the number of microcavities and their geometrical properties, and is independent on the specific trace formed by the entire CROW—a fact that can be used to optimize the chip area deployment.

APPENDIX A: SIMPLIFICATION OF THE ELEMENTS $\langle \mathbf{L}_\Omega \mathbf{H}_M, \mathbf{H}_N \rangle$

We have the following identities [use $(\nabla\times\mathbf{A})\cdot\mathbf{B}=\nabla\cdot(\mathbf{A}\times\mathbf{B})+\mathbf{A}\cdot(\nabla\times\mathbf{B})$, and $\mathbf{A}\cdot(\mathbf{B}\times\mathbf{C})=(\mathbf{A}\times\mathbf{B})\cdot\mathbf{C}$]:

$$\left[\nabla\times\frac{\boldsymbol{\beta}}{\epsilon_r}\times\mathbf{H}_m\right]\cdot\bar{\mathbf{H}}_n=\nabla\cdot\left[\left(\frac{\boldsymbol{\beta}}{\epsilon_r}\times\mathbf{H}_m\right)\times\bar{\mathbf{H}}_n\right]+\left(\frac{\boldsymbol{\beta}}{\epsilon_r}\times\mathbf{H}_m\right)\cdot(\nabla\times\bar{\mathbf{H}}_n), \tag{A1a}$$

$$\left[\frac{\boldsymbol{\beta}}{\epsilon_r}\times\nabla\times\mathbf{H}_m\right]\cdot\bar{\mathbf{H}}_n=-\left(\frac{\boldsymbol{\beta}}{\epsilon_r}\times\bar{\mathbf{H}}_n\right)\cdot(\nabla\times\mathbf{H}_m). \tag{A1b}$$

The inner products in Eq. (3.11) are nothing but volume integrations of the terms above, over arbitrarily large volume V. Using the Gauss theorem, we get for the contribution of the first term on the right-hand side of Eq. (A1a):

$$\int_V\nabla\cdot\left[\left(\frac{\boldsymbol{\beta}}{\epsilon_r}\times\mathbf{H}_m\right)\times\bar{\mathbf{H}}_n\right]d^3x=\oint_{S=\partial V}\left[\left(\frac{\boldsymbol{\beta}}{\epsilon_r}\times\mathbf{H}_m\right)\times\bar{\mathbf{H}}_n\right]\cdot ds\to 0. \tag{A2}$$

This is because the flux through the surface $S=\partial V$ vanishes as V becomes very large (the function $\mathbf{H}_m$ is highly localized within the neighborhood of the mth resonator

and is exponentially decreasing away from it). Therefore, the inner product terms eventually comprises

$$\langle \mathbf{L}_\Omega \mathbf{H}_m, \mathbf{H}_n \rangle = \left\langle \frac{\boldsymbol{\beta}}{\epsilon_r} \times \mathbf{H}_m, \boldsymbol{\nabla} \times \mathbf{H}_n \right\rangle - \left\langle \boldsymbol{\nabla} \times \mathbf{H}_m, \frac{\boldsymbol{\beta}}{\epsilon_r} \times \mathbf{H}_n \right\rangle. \tag{A3}$$

Using again $(\mathbf{A}\times\mathbf{B})\cdot\mathbf{C}=\mathbf{A}\cdot(\mathbf{B}\times\mathbf{C})$,

$$\langle \mathbf{L}_\Omega \mathbf{H}_m, \mathbf{H}_n \rangle = \left\langle \frac{\boldsymbol{\beta}}{\epsilon_r}, \bar{\mathbf{H}}_m \times \boldsymbol{\nabla} \times \mathbf{H}_n \right\rangle - \left\langle \frac{\boldsymbol{\beta}}{\epsilon_r}, \mathbf{H}_n \times \boldsymbol{\nabla} \times \bar{\mathbf{H}}_m \right\rangle. \tag{A4}$$

Since $\boldsymbol{\beta}=\boldsymbol{\beta}(\mathbf{r})=\boldsymbol{\Omega}\times\mathbf{r}/c$, and $\boldsymbol{\Omega}=\Omega\hat{z}$, the above result yields ($\hat{z}\times\mathbf{r}=\rho\hat{\phi}$):

$$\langle \mathbf{L}_\Omega \mathbf{H}_m, \mathbf{H}_n \rangle = c^{-1}\Omega \left\langle \frac{\rho}{\epsilon_r}\hat{\phi}, \bar{\mathbf{H}}_m \times \boldsymbol{\nabla} \times \mathbf{H}_n - \mathbf{H}_n \times \boldsymbol{\nabla} \times \bar{\mathbf{H}}_m \right\rangle. \tag{A5}$$

Note, however, that $\boldsymbol{\nabla}\times\mathbf{H}_n=-i\omega_0\epsilon_0\epsilon_{dn}\mathbf{E}_n$, where $\epsilon_{dn}=\epsilon_d(\mathbf{r}-\mathbf{r}_n)$ is the relative dielectric property of the nth resonator. In the vicinity of the nth resonator, it is identical to the dielectric property ϵ_r of the entire structure. Thus, since $\mathbf{E}_n$ is significant only in this neighborhood, we obtain

$$\langle \mathbf{L}_\Omega \mathbf{H}_m, \mathbf{H}_n \rangle = ic^{-1}\Omega\omega_0\epsilon_0 \langle \rho\hat{\phi}, \bar{\mathbf{H}}_m \times \mathbf{E}_n + \mathbf{H}_n \times \bar{\mathbf{E}}_m \rangle. \tag{A6}$$

B. Z. Steinberg, J. Scheuer, and A. Boag can be reached by e-mail as follows: steinber@eng.tau.ac.il, kobys@eng.tau.ac.il, and boag@eng.tau.ac.il, respectively.

*Also with the Center for Nanosciences and Nanotechnology, Tel Aviv University, Ramat-Aviv, Tel Aviv 69978, Israel.

REFERENCES

1. B. Z. Steinberg, "Rotating photonic crystals: a medium for compact optical gyroscopes," Phys. Rev. E **71**, 056621 (2005).
2. J. Scheuer and A. Yariv, "Sagnac effect in coupled resonator slow light waveguide structures," Phys. Rev. Lett. **96**, 053901 (2006).
3. B. Z. Steinberg, A. Shamir, and A. Boag, "Sagnac effect in rotating photonic crystal microcavities and miniature optical gyroscopes," presented at the Conference on Lasers and Electro-Optics and Quantum Electronics and Laser Sciences (CLEO/QELS), Long Beach, Calif., May 21–26, 2006, paper CWL6.
4. B. Z. Steinberg and A. Boag, "Splitting of microcavity degenerate modes in rotating photonic crystals—the miniature optical gyroscopes," J. Opt. Soc. Am. B **24**, 142–151 (2007).
5. E. J. Post, "Sagnac effect," Rev. Mod. Phys. **39**, 475–493 (1967).
6. O. Painter, J. Vuckovic, and A. Scherer, "Defect modes of a two-dimensional photonic crystal in an optically thin dielectric slab," J. Opt. Soc. Am. B **16**, 275–285 (1999).
7. M. Loncar, M. Hochberg, A. Scherer, and Y. Qiu, "High quality factors and room-temperature lasing in a modified single-defect photonic crystal cavity," Opt. Lett. **29**, 721–723 (2004).
8. T. Shiozawa, "Phenomenological and electron-theoretical study of the electrodynamics of rotating systems," Proc. IEEE **61**, 1694–1702 (1973).
9. J. L. Anderson and J. W. Ryon, "Electromagnetic radiation in accelerated systems," Phys. Rev. **181**, 1765–1775 (1969).
10. H. J. Arditty and H. C. Lefevre, "Sagnac effect in fiber gyroscopes," Opt. Lett. **6**, 401–403 (1981).
11. A. Boag and B. Z. Steinberg, "Narrow band microcavity waveguides in photonic crystals," J. Opt. Soc. Am. A **18**, 2799–2805 (2001).
12. B. Z. Steinberg and A. Boag, "Propagation in photonic crystal coupled-cavity waveguides with discontinuities in their optical properties," J. Opt. Soc. Am. B **23**, 1442–1450 (2006).
13. P. Lancaster and M. Tismenetsky, *The Theory of Matrices*, 2nd ed. (Academic, 1985).